RILEM Technical Letters (2022) 7: 47-57
https://doi.org/10.21809/rilemtechlett.2022.162

Research progress on magnesium silicate hydrate phases and future opportunities

Ellina Bernard [1,o,*]

[1] Empa Swiss Federal Laboratories for Materials Science and Technology, Switzerland

[o] Ellina Bernard was invited for submission of this letter as an awardee of the Gustavo Colonnetti Medal granted by RILEM in 2022

Received: 01 June 2022 / Accepted: 21 August 2022 / Published online: 01 September 2022
© The Author(s) 2022. This article is published with open access and licensed under a Creative Commons Attribution 4.0 International License.

Abstract

This short letter summaries the latest research on the structure and thermodynamic modelling of the magnesium silicate hydrates (M-S-H) phases. M-S-H structure is comparable to hydrated clays, with a smaller and rounder microstructures compared to clay platelets. Similar to clay minerals, M-S-H can incorporate ions such as aluminium and hydrated exchangeable cations to compensate the negative surface charge. This fundamental understanding of M-S-H structure allowed to develop structure-based thermodynamic models, which can further help to optimise the conditions for M-S-H formation and its use as cementitious materials. Optimized binders containing M-S-H have the advantages of presenting: i) good mechanical properties, ii) dense microstructure and potentially good resistances to leaching and iii) low pH values. These types of binders could therefore be used for cement products with non-steel reinforcement, for the encapsulation of specific wastes, for products containing natural fibres or for the clay stabilisation, etc.

Keywords: Magnesium silicate hydrate (M-S-H); Structure; Surface charges; Low pH cements

1 Introduction

Magnesium enrichment is often observed during the natural degradation processes of concrete in contact with river or saline waters (see e.g. [1-10]). Although this Mg enrichment has often been attributed to the precipitation of $Mg(OH)_2$ (brucite) solely, also magnesium silicate hydrate (M-S-H) can precipitate. The leaching of Ca-phases, which is one of the main degradation mechanism of cementitious materials, leads to the dissolution of calcium silicate hydrate (C-S-H) and the release of amorphous silica [11]. C-S-H, with its characteristic silicate chains as the typical dreierketten structure [12] is stable at pH values down to 9.5-10.0. Depending on the availability of Mg^{2+} and the pH values of the environment, M-S-H forms from the amorphous silica and from the available Mg^{2+} [13]. M-S-H has long been considered to be similar to C-S-H [14], and as a non-cementitious product of the seawater degradation of Ca-based cement [15-18]. However, M-S-H phases have a layered silicate structure [19], fundamentally different to the silicate chain structure of C-S-H [20]. In addition, M-S-H is stable over a larger pH range and at significantly lower pH values [21].

M-S-H is the sole hydrate of reactive MgO and silicate cements. Phosphates can used as superplasticizer reducing the amount of water needed to achieve a good workability [22]. Additionally, the phosphates act as accelerator to the reaction resulting in faster M-S-H formation [22, 23] and help to obtain good compressive strength to the M-S-H matrix after 28 days (~50-80 MPa) [22, 24]. The interest in M-S-H as the main component of cementitious materials grew in the last decades due to the low pH of the cement [25, 26]. Such low pH cements are of interest for radioactive waste management for radionuclide retention [27-29], or to deal with radioactive wastes as the encapsulation of nuclear magnox sludges [30] and problematic nuclear aluminium wastes [31]. Moreover, it is also interesting for other applications where low pH binders are required, e.g. for the use of natural fibres [32, 33].

Reactive Mg-cements based on Mg-rich materials derived from common Mg silicate rocks (MOMS) have the potential to sequester CO_2 in the form of stable carbonates [34], meaning such cements can exhibit a net negative CO_2 emission (i.e., capable of CO_2 mineralisation). This type of cements are still at an early research-state. They are mainly composed of hydrated magnesium carbonates (HMC) and feature good mechanical properties (20 MPa to 50 MPa) [26, 35]. If SiO_2 as a by-product of separating reactive MgO from the Mg silicate minerals, is added the formation of M-S-H is observed [36]. The formation of the interconnected HMC and M-S-H should lead to a denser microstructure [37, 38] and therefore better mechanical performance, but this requires more investigations.

A detailed knowledge on the performance and specifically the durability in different environments of such binders containing different amount of M-S-H and HMC cements are

*Corresponding authors: Ellina Bernard, ellina.bernard@empa.ch

mandatory for further development of such binders. Because of the long timescales needed to carry out durability tests, thermodynamic calculations might be used to predict the long-term stability of these phases in different environment conditions.

This short letter summaries the latest research on the structure of M-S-H and recent thermodynamic data, complemented by new thermodynamic calculations and highlights potential applications of such layered-type phases.

2 Structure and formation of M-S-H

2.1 Structure of M-S-H

The silicates in the M-S-H phases are arranged in tetrahedral layers as in phyllosilicate minerals as observed by ^{29}Si MAS NMR studies by the presence of Q^2 and Q^3 signals while magnesium is present in octahedral layers as commonly observed in $Mg(OH)_2$ (brucite) [19]. The phyllosilicates present 3 typical arrangements of the tetrahedral Si-O layers and the octahedral Al-O, Fe-O or Mg-O layers:

i. T:O i.e. one tetrahedral layer over one octahedral layer corresponding to a 1:1 layer silicate structure as in the serpentines (e.g. chrysotile, antigorite, lizardite),

ii. T:O:T corresponding to a 2:1 configuration, i.e. two tetrahedral layers sandwiching an octahedral layer as in talc or

iii. T:O:T-O corresponding to a 2:1 configuration with an extra positively charged brucite layers as in chlorite.

M-S-H seems to include all of the above arrangements and its structure is comparable to hydrated precursors sepiolite [39], nano crystallite hydrated of talc [19, 40], ill-defined chemical hydrated antigorite [40, 41], lizardite [30, 42], stevensite [40] or saponite [9, 19, 41].

Although M-S-H presents similarities with hydrous phyllosilicates, the coherent particle size of M-S-H is much smaller. X-rays diffraction (XRD) patterns of M-S-H indicate that the M-S-H has only nanometer-sized coherent scattering domains (1.5 nm in the ab plane, and 2.4 nm along c axis), which causes the broad reflections in the XRD pattern [19] (see Fig. 1a and b). The mean basal spacing (Fig. 1a and c) gradually decreases from 12 Å to 10 Å with the increase of the Mg/Si from 0.9 to 1.3 indicating potentially that the solid solution is an intermix of T:O and T:O:T nanocrystallite depending on the Mg/Si ratio.

X-ray pair distribution function (PDF) calculations confirmed that M-S-H phases have a relatively short coherence length (1.2 nm) [41]. Similarly, Chiang et al. [43] suggested a spherical structure for M-S-H with an average radius of 1.7±1 nm based on SAXS measurement. Finally, also N_2-sorption measurements suggested a very small particle size with surface area calculated by BET above 200 m^2/g on samples synthesised in suspension [41] and in pastes [44].

As much as M-S-H has similarities to phyllosilicates, it is rather a precursor of them presenting a variable composition and a variable structure (mixture of T:O and T:O.T), i.e. a solid-solution with Mg/Si ratios ranging from 0.75 to 1.5 [40, 45]. A schematic sketch for the structure of M-S-H is given in Fig. 2.

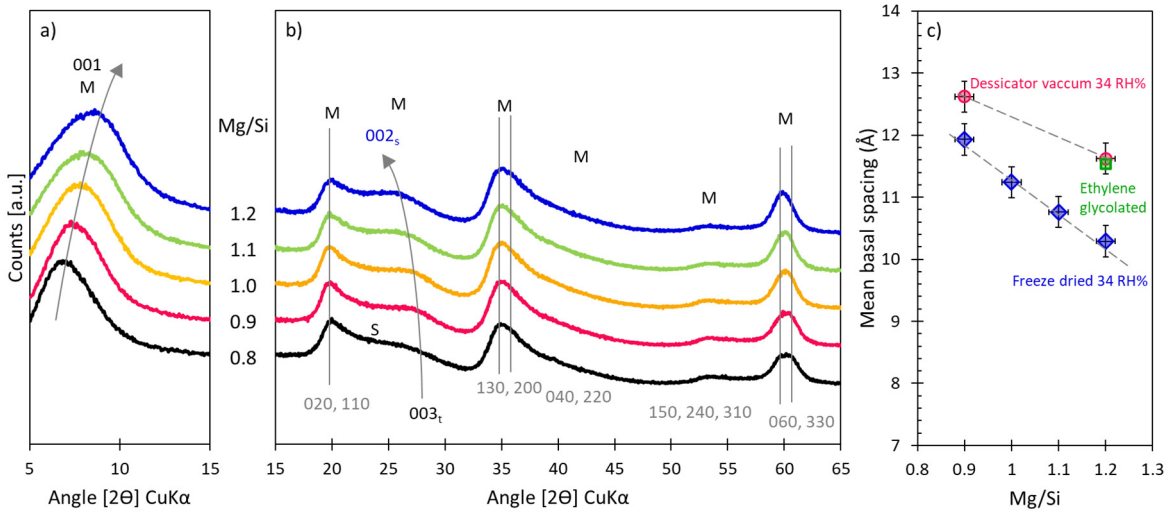


Figure 1. a) and b) XRD patterns (indexed following the crystal structure of talc (=t), serpentine (=s) and Mg-swelling clays (=M)), c) Mean basal spacing (layer-to-layer distance) measured from XRD patterns as a function of Mg/Si in M-S-H. Freeze dried=freeze dried samples and re-equilibrated to 34RH% over $CaCl_2$, desiccator vacuum=directly dried over $CaCl_2$ 34RH% in a vacuumed desiccator.

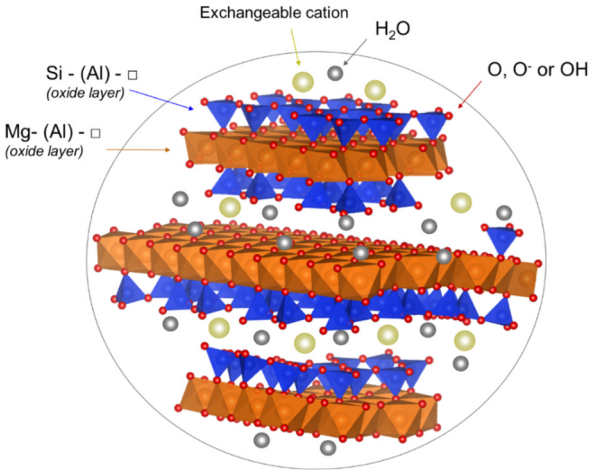


Figure 2. Potential schematic sketch for the structure of M-(A-)S-H based on the structural information from [9, 19, 21, 41-43, 46]. Details on the surface of M-S-H is given in Fig. 4.

M-S-H contains also a large amount of water, between 1.5 and 4 H_2O/Mg based on numerous TGA measurements [19, 25, 40, 41, 47]. An example of a typical TGA is given in Fig. 3. This water is present both as i) poorly bound water, i.e. water molecule physically sorbed on the surface (monolayer, multilayers and/or in the interlayer) and ii) within the structure as a water molecule and hydroxyl groups bound to silicon and magnesium, in inner and surface positions [41]. While the amount of hydroxyl groups is constant at different relative humidity [41], the content of water in the M-S-H varies with the poorly bound water and is strongly related to the relative humidity [41, 48].

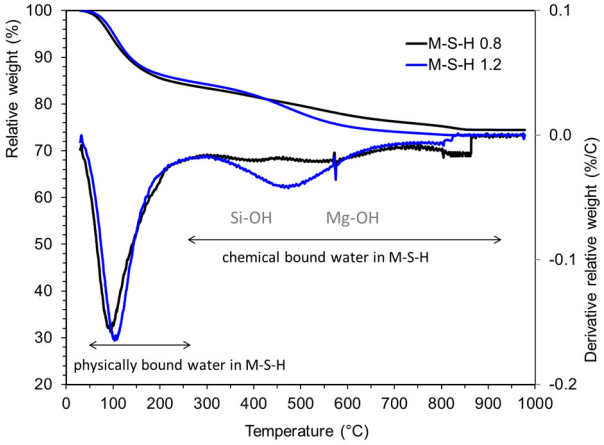


Figure 3. Thermogravimetric analysis on typical M-S-H (adapted from [41]).

The large amount of water, particularly the poorly bound water, and the swelling (see Fig. 1c) in the particles distinguishes the M-S-H from typical hydrous phyllosilicates such as talc, antigorite or sepiolite but related the M-S-H to the smectite mineral group. Trioctahedral smectite as saponite:

$(Ca_{0.5}Mg_{0.5}Na{\cdot}nH_2O)_x\,Mg_3[(Si,Al)_4O_{10}]\,(OH)_2{\cdot}mH_2O)$,

and/or dioctahedral smectite as montmorillonite:

$(NaCa_{0.5}{\cdot}nH_2O)_x(Al,Mg,□)_2\,[Si_4O_{10}](OH)_2{\cdot}mH_2O$,

where □ is a vacant site, contain a much larger amount of water and swell depending on the relative humidity. This is due to the uptake of hydrated cations in the interlayers to compensate the negative surface charge, as typical for smectites. The negative surface charge usually originates from the substitution of Si and/or Mg by Al in the tetrahedral and/or octahedral sheets. Saponite and montmorillonite are typical trioctahedral and dioctahedral smectites, where Al is incorporated only in the silicate tetrahedral or only in the magnesia octahedral layers, respectively. Only vermiculite contains aluminium in both octahedral and tetrahedral layers:

$(Ca_{0.5}Mg_{0.5}Na{\cdot}nH_2O)_x(Mg,Al,□)_3\,[(Al,Si)_4O_{10}](OH)_2{\cdot}\,mH_2O$,

where □ is a vacant site. SEM/EDS data of the surface of degraded cement pastes tend to indicate that aluminium can be present either in the M-S-H similar to smectites or bound in hydrotalcite [7, 9, 49]. Laboratory experiments confirm that magnesium silicate hydrate containing aluminate or magnesium alumino silicate hydrate (M-A-S-H) can form from co-precipitation of MgO, SiO_2 and metakaolin or $NaAlO_2$ with rather low aluminium content (maximum Al/Si ≈ 0.15). The incorporation of Al in tetrahedral SiO_2 layers and potentially in the octahedral layers in M-S-H has been established by ^{27}Al MAS NMR [46, 50]. On the same co-precipitated samples, Vespa et al. [51] confirmed by X-ray absorption near-edge spectroscopy the presence of Al in the tetrahedral and octahedral layers of M-S-H.

A limited amount of Al can be taken up in M-S-H resulting in the formation of M-(A-)S-H. In the presence of more aluminium, in addition Mg-Al layered double hydroxide phases are observed for instance in a PC blended with reactive MgO/SiO_2 [52]. Similarly, hydrotalcite precipitates together with the N-A-S-H gel (or zeolitic precursors) in alkali activated slags rich in Mg and Al (see e.g. [53-57]). Hydrotalcite and zeolites were also observed in MgO and SiO_2 cements containing a high $NaAlO_2$ content [57], while at low amounts of $NaAlO_2$ and pH values below 10, no zeolites were observed, only hydrotalcite/$Al(OH)_3$ [50]. In any cases, the presence of extra Al-containing phases limited the Al incorporation in M-S-H. Also Jia et al. [58] observed a limitation of Al/Si (< 0.05) in M-A-S-H in the presence of aluminium nitrate in the MgO-SiO_2 system. In most of the cases, the exact incorporation of Al in M-A-S-H is extremely difficult to quantify due to the nanocrystallinity of the Al-containing phases, either Al-hydroxides, hydrotalcite-like phases, N-A-S-H gels or M-A-S-H.

The similarities with saponite, one of the trioctahedral smectites containing exchangeable cations, indicates that also M-S-H should have exchangeable cations in the interlayer or at the surface of the silicate layers. In fact, M-S-H and M-A-S-H show a negative surface charge [41, 46], but a rather low cation exchange capacity (CEC) of about 30-40 meq/100g at pH between 8 and 10.5, compared to smectites with 80-200 meq/100g [59]. Usually, the CEC of smectite is related to the incorporation of Al in the tetrahedral layers (Al^{3+} replacing Si^{4+}) or in the octahedral layer (Al^{3+} and vacant site replacing Mg^{2+}).

Therefore the CEC is directly related to the amount of Al in the smectite structure. The CEC in M-(A-)S-H is independent of the presence of Al in the structure, which could be related to the incorporation of Al in both octahedral and tetrahedral layers without vacant site or a CEC mainly related to the external surface charge of the M-(A-)S-H particle [46]. However, the CEC of M-S-H increases strongly with the pH and can reach 150 meq/100g for pH values of ~12.5 [21]. This indicates that the CEC in M-S-H is more related to the deprotonation of the structural hydroxyl groups than to the incorporation of Al in the structure. The deprotonation of the surface of M-S-H with increasing pH and its charge compensation by hydrated cations is schematically represented in Fig. 4. M-S-H takes up also monovalent cations [21, 29], although mainly at the exchangeable sites and not within the main layer [21, 51]. The uptake of Mg on exchangeable surface site is very small due to the low Mg concentrations in solution at pH values above 10.5 [41]. However, the presence of carbonates in solution leads to the formation of aqueous Mg-carbonate complexes, which increase the Mg concentration as well as the Mg uptake at the exchangeable surface sites [45].

Natural montmorillonite and saponite usually have a significant fraction of Ca^{2+} at the cation exchange sites (e.g. [60]). Ca^{2+} uptake is preferred over the uptake of K^+ or Na^+ due to the better affinity of the surface sites for divalent cations, but also due to the often low Mg concentrations in the environment when the clay minerals are forming. The presence of Ca on the cation exchange sites was also observed for synthetic M-S-H [61, 62]. M-S-H showed also a strong immobilization capacity for the secondary metal cations [28, 29], although the long-term uptake and stability has not been investigated.

2.2 Formation of M-S-H, stability and competition with brucite formation

In geology, the occurrence of M-S-H is observed due to the serpentinization of olivine-rich rocks. This weathering phenomenon leads to brucite formation and to a high pH of the equilibrium solution, which leads to a partial dissolution of quartz and results in dissolved Mg and Si, ready to react into M-S-H [63].

Similar dissolution-precipitation reactions due to an increased pH happen also at the interaction zone of clayey and cementitious materials: i) the clayey materials release some Mg, either from the cation exchange sites of the clays or by partial dissolution of dolomite [10], ii) the low pH of the clayey pore solution leads to the dissolution of C-S-H and of silica [11, 64], iii) the pH at the interface between clay and cements provides the right medium for the precipitation of M-S-H [7, 65], which occurs even at very low Mg concentrations.

The same mechanism is also occurring during the hydration of MgO and silica fume (in concrete or suspension), with first the formation of $Mg(OH)_2$ from MgO, which subsequently reacts with the amorphous silica to M-S-H phases [25, 66]. Many laboratory experiments observed a very slow M-S-H formation over months to years [25, 47, 66, 67]. The magnesium hydroxide dissolves slowly in the presence of M-S-H, potentially slowed down by the presence of silicon in the solution which kinetically hinders brucite dissolution [66, 68]. It takes up to 6 months for initially precipitated magnesium hydroxide to completely react to M-S-H at Mg/Si=1 [47] and two years to obtain M-S-H with Mg/Si=1.3 [66]. Reaction kinetics accelerate with increasing temperature, also due to the slightly lower stability of brucite at elevated temperature [39, 47, 66].

The Mg concentration calculated by thermodynamic modelling in the presence of carbonates or phosphates is presented in Fig. 5. It was recently observed that dissolved carbonates also speed up the formation of M-S-H [69] by increasing the concentration of Mg due to the formation of aqueous complexes [45], as detailed in Fig. 5. Additionally, higher Mg/Si ratios of up to 1.5, as in serpentine group minerals, can be observed in presence of carbonates [45], which were not reached otherwise, not even after a 3-year-equilibration at 20°C, or 2-year-equilibration at 50°C [41]. Promising mechanical properties can be reached with carbonates as accelerator [45].

Also the formation of M-S-H in hydrated cement paste in the presence of phosphate was studied in [22, 23, 30, 70], showing faster precipitation of M-S-H than in suspension without phosphates. Jia et al. [70] suggested that the phosphate hinders the formation of $Mg(OH)_2$ during the hydration of MgO by forming protective layers composed of $6(MgOH)^+(PO_3)_6^{6-}$ on the MgO surface. They also observed a strongly increased Mg concentration in the presence of phosphate [70]. It can be seen in Fig. 5 that both carbonate and phosphate increase the dissolved magnesium for pH values above 9.5. For pH above 11-11.5 the presence of phosphate leads to stronger complex formation, increasing the total Mg concentration in solution. This would lead to a faster formation of M-S-H, while at lower pH (between 9.5 and 11) the carbonate complexes increase the dissolved Mg and results in higher Mg concentration for the faster formation of M-S-H. Note that the model predicts the precipitation of Bobierrite ($Mg_3(PO_4)_2$-$8H_2O$) for pH below 11.8. In Fig. A1 a model is given where its formation was prevented. The presence of organic as acetate showed a faster reaction of brucite into hydrated magnesium carbonates phases (HMC) [71, 72], although the organics do not significantly change the Mg concentrations [73].

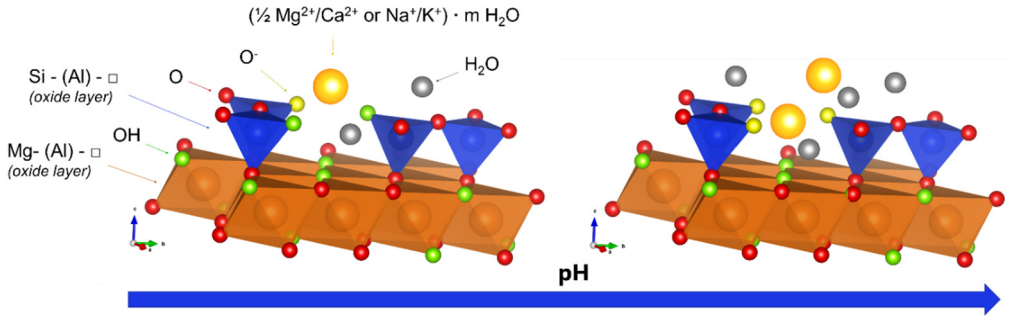


Figure 4. Schematic sketch for the surface of M-S-H where defects are occurring. With the increase of pH, the hydroxyl groups (green) are deprotonated (yellow) and more exchangeable cations are in the surrounding of the layers.

While developing M-S-H cement, it was shown that sodium phosphate was an excellent dispersant and acted as superplasicizer [30]. Although the phosphates are limited and expensive, the use of carbonates to accelerate M-S-H formation will be cheaper and more sustainable. Additionally, Walling et al. [30] observed a retarded formation of M-S-H above 2 wt% of phosphate. This could be due to i) the passivation of the MgO surface by phosphates, which limits the dissolution of MgO, and therefore the dissolved Mg to form M-S-H or due ii) strong Mg-phosphate complexes that slow down the formation of Mg-silicate as precursors of M-S-H.

3 Thermodynamic databases

Thermodynamic modelling approaches have been used for at least 15 years to understand phase formation and the reaction processes involved in cement paste hydration [74]. In 2015, Roosz et al. [19] presented thermodynamic data assuming the formation of two single M-S-H phases with Mg/Si= 0.6 and 1.2, while Nied et al. [40], in 2016, published the first solid solution model for M-S-H with Mg/Si between 0.75 and 1.5 more appropriated to the experimental data. The ion activity product of M-S-H observed in the solution decreases with time due to the slow formation of M-S-H [75] and approaches the solubility products of talc or serpentine in the long-term [66]. In this letter, the thermodynamic modelling was carried out using the Gibbs free energy minimization program GEMSelektor [76] combined with the GEMS-PSI thermodynamic database [77] and the cemdata2018 database [78]. These databases were completed with thermodynamic data from [40, 46, 62] to describe the Ca and Al uptake in M-S-H: (C-)M-(A)S-H, the uptake of different anions in hydrotalcite from [79], the possible formation of (hydrated) magnesium carbonates [45] and Mg-phosphates phases and complexes from [80]. The modelling were used to predict the stability domains of M-S-H and M-A-S-H in the absence and presence of carbonates.

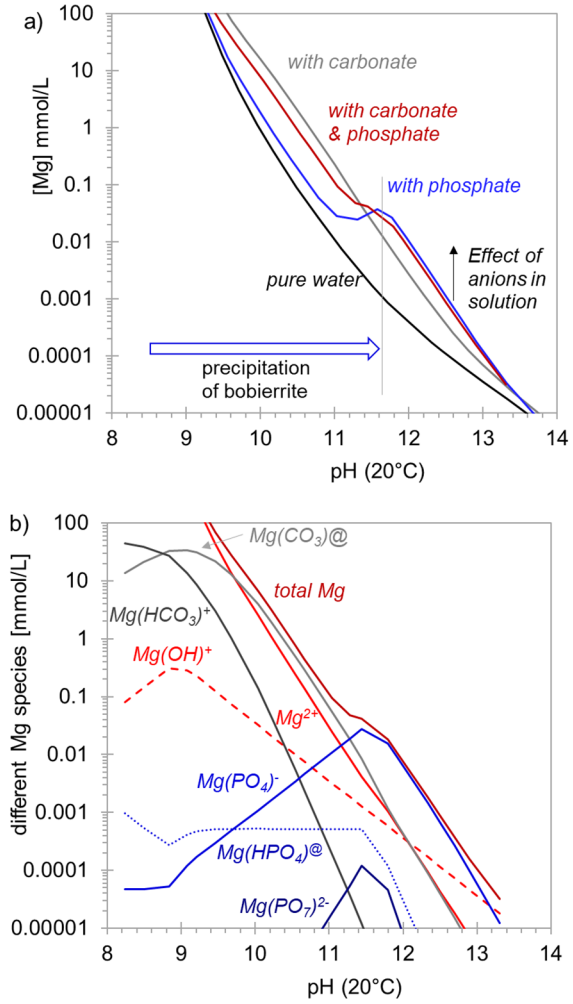


Figure 5. a) Modelled brucite solubility curves in pure water and in carbonated solution ($CO3^{2-}$ = 80 mmol/L) and with phosphate (3 wt. % of NaHMP), b) different Mg species associated to the solubility of brucite in carbonated and phosphate solution ($CO3^{2-}$ = 80 mmol/L and 3 wt. % of NaHMP). Adapted from [45].

4 Stability of M-(A-)S-H

4.1 Stability of M-S-H vs. C-S-H

As detailed above, M-S-H can form from the degradation of the C-S-H in hydrated Portland cement paste. Fig. 6 shows the stability domains of M-S-H (Mg/Si=1) and C-S-H (Ca/Si=1) in the pH range 6 to 14. M-S-H is thermodynamically stable from pH 7 to 14. Between pH 9 and 11.5, only M-S-H is predicted, while at lower pH values silica forms and brucite at higher pH values, such that the M-S-H composition varies from low to high Mg/Si with pH. The formation of M-S-H decreases the Mg and Si concentrations in solution compared to brucite or amorphous silica. In contrast, C-S-H is only stable at high pH values and destabilizes at pH values below ~9.

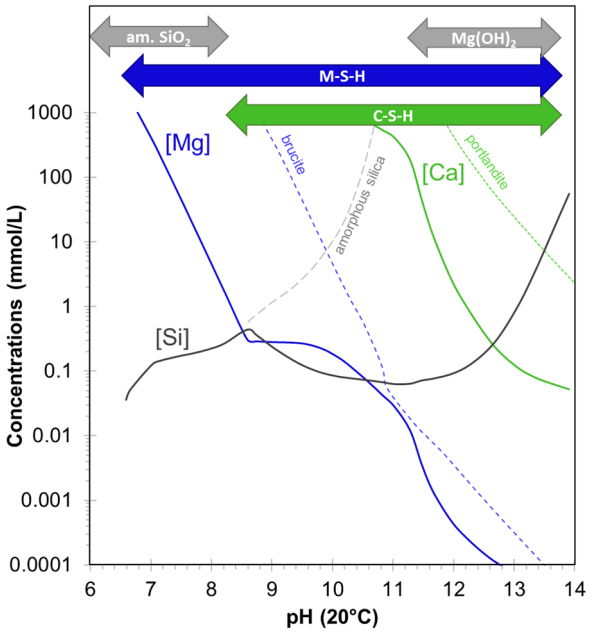


Figure 6. Calculated stability of M-S-H (Mg/Si=1) and C-S-H (Ca/Si=1) and calculated Mg, Ca and Si concentrations between pH 6 to 14. The solubility of brucite, portlandite and amorphous silica are added (as dotted lines for comparison).

4.2 M-(A-)S-H stability in presence in aluminate

In presence of Al, magnesium silicate hydrates containing aluminate or magnesium alumino silicate hydrate (M-A-S-H) can form. However, assessing the incorporation of Al in M-A-S-H is experimentally difficult due to the nanocrystallinity of the Al-containing phases.

The incorporation of Al in the M-S-H can be approximated by using the ion activity products (IAPs) (calculated in [46]) and assuming an ideal solid solution with M-S-H [40]. Fig. 7 shows the dissolved Al, Mg and Si as a function of the Al/Si for a) Mg/Si ~1 and b) Mg/Si ~1.5, compared with the few measured data available in the literature [46]. The model predicts the total incorporation of Al up to Al/Si=0.2 in M-(A-)S-H for Mg/Si=1, while the precipitation of microcrystalline $Al(OH)_3$ is predicted above Al/Si=0.15 for M-(A-)S-H with Mg/Si=1.5.

In the presence of sodium carbonate (17 g/L), the models predict the formation of hydrotalcite-like phase containing carbonates instead of microcrystalline $Al(OH)_3$ and the precipitation of zeolites, at higher Al contents. This is consistent with the literature where the carbonated hydrotalcite is the more stable than OH-hydrotalcites [81, 82]. In presence of phosphate, P-hydrotalcite might also form [83]. This indicates that the carbonates/phosphates in presence of aluminates lead certainly to a faster formation of M-(A-)S-H but also, to the formation of hydrotalcite and in theory, a decreased amount of M-(A-)S-H in the system.

4.3 M-(A-)S-H stability vs. carbonates phases

M-S-H together with calcite and/or gypsum has been observed as a degradation product of Ca-based cement [3, 16]. Under such conditions, also magnesite ($MgCO_3$) would be stable. However, its formation at room temperature is kinetically hindered and unlikely, while calcite crystallises much faster than magnesite [84]. A range of different hydrated magnesium carbonates (HMCs) exist as summarised in Fig. 8. Some of them are mostly likely to form at room conditions. HMCs have gained attention as an alternative to PC and for their potential for carbon capture [85]. Such HMC cements are still at an early research stage, but they already feature promising mechanical properties (compressive strength between 20 and 50 MPa) [26, 37]. The hydration of MgO blended with hydromagnesite ($Mg_5(CO_3)_4(OH)_2 \cdot 4H_2O$) shows the formation of HMC products, some poorly crystalline brucite and adequate compressive strength [26, 35]. The utilisation of Mg-acetate accelerated the formation of HMCs, lead to a higher carbonation degree [71] and stabilise the hydrated Mg-carbonates phases [72].

As detailed above, the carbonates play an important role in the formation of M-S-H. However, the stability of M-S-H versus the stability of HMC is not really understood and only few experimental studies have been published. It was recently shown that MgO/SiO_2 blended with hydromagnesite forms mainly M-S-H and that hydromagnesite partially reacts into M-S-H [45] indicating that M-S-H are more stable than hydromagnesite.

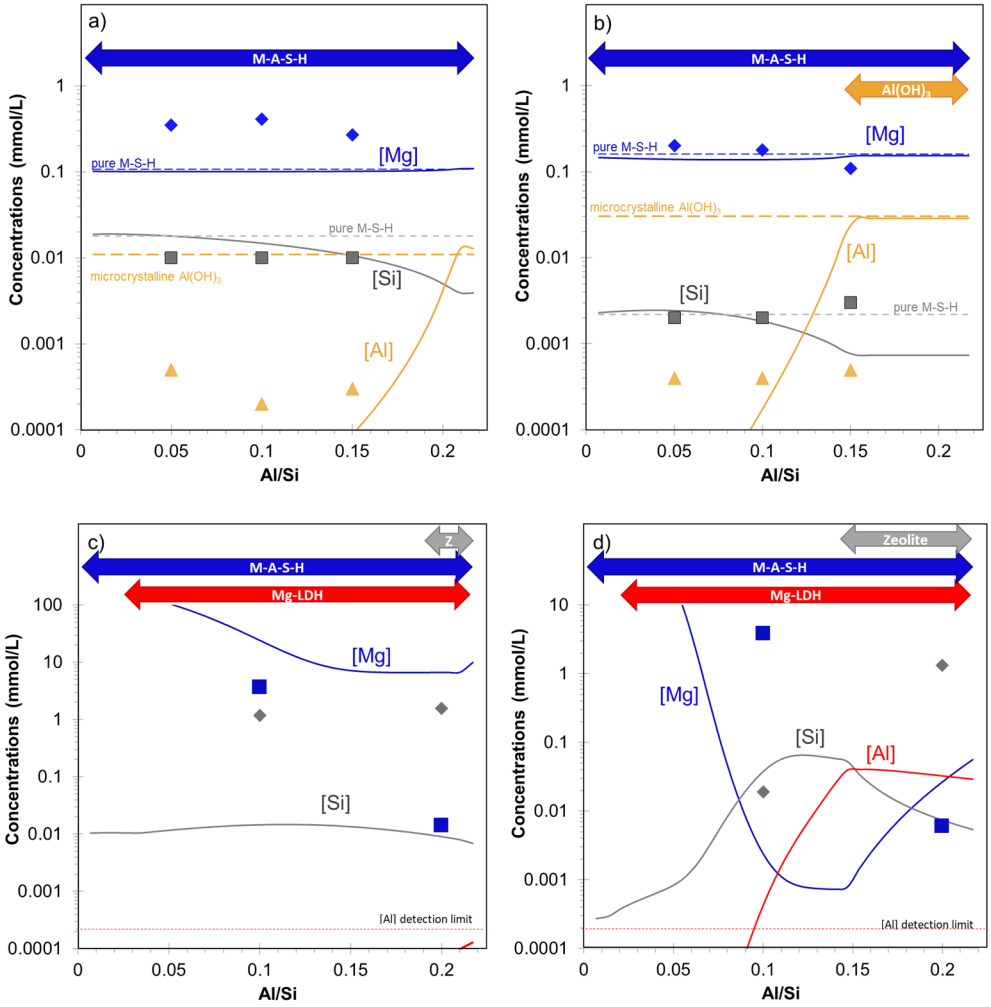


Figure 7. Calculated solubility curves for M-(A-)S-H compared to the available experimental data [46, 50] for a) and c) Mg/Si ~1 b) and d) Mg/Si ~1.5, c) and d) containing Na_2CO_3 in the system, using M-A-S-H solid solution [46] and hydrotalcite solid solution [79]. Solubility without the Al incorporation in M-A-S-H, and the formation of $Al(OH)_3$ are indicated by dotted lines.

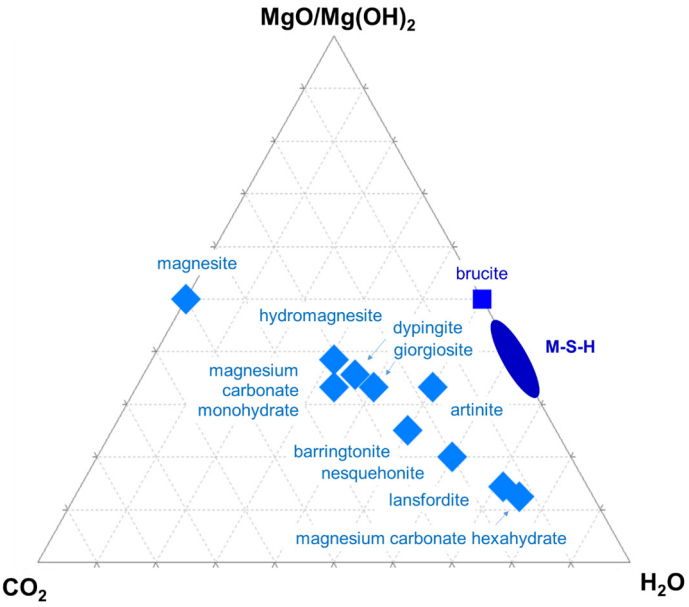


Figure 8. MgO-CO_2-H_2O ternary plots based on the composition of the different magnesium carbonates and M-S-H phases (silica is only present in M-S-H). Adapted from [45].

5 Conclusions and opportunities

To sum up, M-(A-)S-H forms in many geological environments despite the small amount of Mg available in those systems likely indicating a good stability over time. M-(A-)S-H phases have been observed to form and are calculated to be stable at pH values between 7.5 and 12.5 [11, 21, 45, 46]. M-(A-)S-H can be considered as a precursor of hydrated Mg-clay minerals. The optimum conditions of M-(A-)S-H formation can be obtained from the recent thermodynamic data available in literature.

Additionally, good mechanical properties of M-S-H-based binders can be reached in presence of phosphates or carbonates. The use of phosphate seems problematic due to environmental issues, but also carbonates seem to act as efficient accelerators. Unluer 's team recently looked at using M-S-H binders for 3D printed building components and showed that specific mixes of M-S-H/brucite exhibited thixotropic behaviour [86]. As such, they are usuable for this purpose based on their rheological and mechanical properties. M-S-H based mortars also show a good resistance to penetration by chloride ions [87]. But more systematic experimental and modelling studies on the mechanical and durability properties are required.

The formation of M-S-H could also improve the mechanical properties of hydrated magnesium carbonate (HMC) cements. However, there is a lack of experimental studies and the available databases do not (yet) permit the modelling of the type of hydration/carbonation system [45].

The use of calcined clay instead of micro silica could decrease the price of such building materials. Additionally, the combination of MgO with a reactive aluminosilicate, such a calcined clays, has been recently considered as an alternative binder [46, 88-92]. Clays are widely available in the Earth's crust [93] compared to the availability of silica fume [94, 95] and they can be activated to produce large amount of reactive aluminosilicates. Shah et al. [91, 92] showed that the MgO-metakolin presents better mechanical performance due to the formation of hydrotalcite in addition of M-S-H which lowers the porosity of the matrix. However, currently very little is known of the chemistry involved in Al containing Mg-cement indicating that more research needs to be conducted on this topic. For example, the formation of hydrotalcite is not yet clearly understood and no data on the interaction with the accelerators are available. The development of a consistent and complete thermodynamic database for the Mg-containing phases potentially precipitating in Mg-binders would improve the understanding.

Although the production process of Mg-based binders is not yet optimized. If the environmental impact can be lowered, Mg-based binders have a high potential to partially replace Portland based cement for specific purposes such as cement products with non-steel reinforcement where a high pH is not mandatory for the passivation of the steel. Low pH matrices are also more adapted for the encapsulation of specific wastes, for products containing natural fibres (e.g. for insulation) or for the clay stabilisation in order to avoid the degradation of wastes, natural fibres or clay minerals by the high pH environment.

Acknowledgments

I would like to sincerely thank Barbara Lothenbach, and the Empa Team of the Laboratory for concrete and asphalt, particularly Alexander German, Frank Winnefeld and Hoang Nguyen for the discussion about Mg-binders. Isabelle Pochard, Celine Cau-Dit-Coumes, Alexandre Dauzères and Fabien Le Goff for accompanying me on my journey to study synthetic M-S-Hs during my PhD Work. I would like to acknowledge Urs Mäder and Andreas Jenni (University of Bern) for all the discussions about the interface between cementitious materials and clays, Daniel Rentsch for NMR discussions and analyses. Rupert Myers and Marcus Yio for the support during my time at Imperial College. The research leading to these results has received funding from IRSN, the European Union's Horizon 2020 Research and Training Programme of the European Atomic Energy Community (EURATOM) (H2020-NFRP-2014/2015) under grant n◦ 662147 (CEBAMA) and the Swiss National Science Foundation (SNSF) for Postdoc mobility Fellowship under the grant n◦ P400P2_194345 and Ambizione Fellowship under the grant n◦ PZ00P2_201697.

Appendix

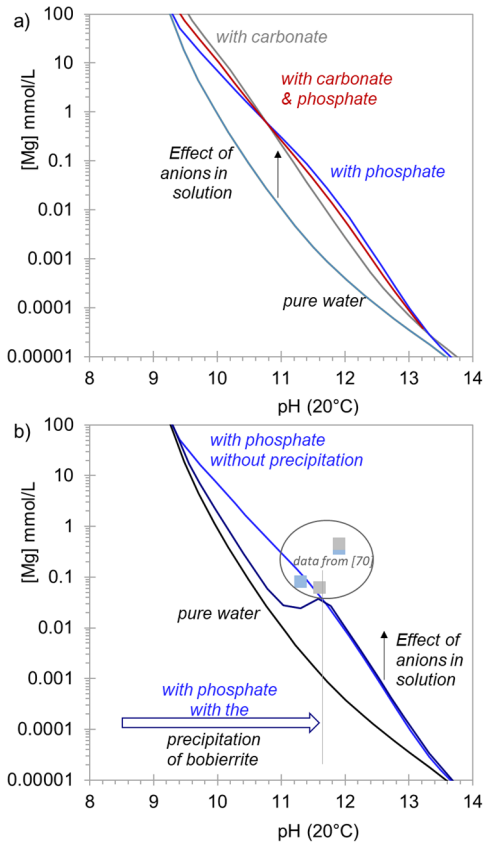


Figure A1. a) Brucite solubility curves in pure water and in carbonated solution (CO_3^{2-} = 80 mmol/L) and with phosphate (3 wt.% of NaHMP) (Mg-phosphate phase precipitations excluded) b) comparison with data in literature ([70] after 1 and 10 days of reaction, phosphate (0.5 and 2 wt.%)).

References

[1] D. Bonen, M.D. Cohen, Magnesium sulfate attack on portland cement paste-II. Chemical and mineralogical analyses, Cem Concr Res, 22 (1992) 707-718. https://doi.org/10.1016/0008-8846(92)90023-O

[2] M. Santhanam, M.D. Cohen, J. Olek, Mechanism of sulfate attack: a fresh look: part 1: summary of experimental results, Cem Concr Res, 32 (2002) 915-921. https://doi.org/10.1016/S0008-8846(02)00724-X

[3] K. De Weerdt, H. Justnes, The effect of sea water on the phase assemblage of hydrated cement paste, Cem Concr Compos, 55 (2015) 215-222. https://doi.org/10.1016/j.cemconcomp.2014.09.006

[4] U.H. Jakobsen, K. De Weerdt, M.R. Geiker, Elemental zonation in marine concrete, Cem Concr Res, 85 (2016) 12-27. https://doi.org/10.1016/j.cemconres.2016.02.006

[5] M. Rosenqvist, A. Bertron, K. Fridh, M. Hassanzadeh, Concrete alteration due to 55 years of exposure to river water: Chemical and mineralogical characterisation, Cem Concr Res, 92 (2017) 110-120. https://doi.org/10.1016/j.cemconres.2016.11.012

[6] A. Jenni, U. Mäder, C. Lerouge, S. Gaboreau, B. Schwyn, In situ interaction between different concretes and Opalinus clay, Physics and Chemistry of the Earth, Parts A/B/C, 70 (2014) 71-83. https://doi.org/10.1016/j.pce.2013.11.004

[7] A. Dauzères, G. Achiedo, D. Nied, E. Bernard, S. Alahrache, B. Lothenbach, Magnesium perturbation in low-pH concretes placed in clayey environment - solid characterizations and modeling, Cem Concr Res, 79 (2016) 137-150. https://doi.org/10.1016/j.cemconres.2015.09.002

[8] J.L. Garcia Calvo, A. Hidalgo, C. Alonso, L. Fernández Luco, Development of low-pH cementitious materials for HLRW repositories: Resistance against ground waters aggression, Cem Concr Res, 40 (2010) 1290-1297. https://doi.org/10.1016/j.cemconres.2009.11.008

[9] C. Lerouge, S. Gaboreau, S. Grangeon, F. Claret, F. Warmont, A. Jenni, V. Cloet, U. Mäder, In situ interactions between Opalinus Clay and Low Alkali Concrete, Physics and Chemistry of the Earth, Parts A/B/C, 99 (2017) 3-21. https://doi.org/10.1016/j.pce.2017.01.005

[10] U. Mäder, A. Jenni, C. Lerouge, S. Gaboreau, S. Miyoshi, Y. Kimura, V. Cloet, M. Fukaya, F. Claret, T. Otake, M. Shibata, B. Lothenbach, 5-year chemico-physical evolution of concrete-claystone interfaces, Swiss Journal of Geosciences, 110 (2017) 307-327. https://doi.org/10.1007/s00015-016-0240-5

[11] E. Bernard, B. Lothenbach, F. Le Goff, I. Pochard, A. Dauzères, Effect of magnesium on calcium silicate hydrate (C-S-H), Cem Concr Res, 97 (2017) 61-72. https://doi.org/10.1016/j.cemconres.2017.03.012

[12] I.G. Richardson, The calcium silicate hydrates, Cem Concr Res, 38 (2008) 137-158. https://doi.org/10.1016/j.cemconres.2007.11.005

[13] K. De Weerdt, E. Bernard, W. Kunther, M.T. Pedersen, B. Lothenbach, Long-term performance of cementitious materials exposed to saline solutions Cem Concr Res, submitted (2022).

[14] S. Diamond, W.L. Dolch, J.L. White, Studies on Tobermorite-Like Calcium Silicate Hydrates, Technical Paper, Purdue University Lafayette Indiana, 33 (1963). https://doi.org/10.5703/1288284313642

[15] O. Al-Amoudi, Rasheeduzzafar, M. Maslehuddin, S. Abduljauwad, Influence of chloride ions on sulphate deterioration in plain and blended cements, Magazine of Concrete Research, 46 (1994) 113-123. https://doi.org/10.1680/macr.1994.46.167.113

[16] M. Santhanam, M.D. Cohen, J. Olek, Mechanism of sulfate attack: a fresh look: Part 2. Proposed mechanisms, Cem Concr Res, 33 (2003) 341-346. https://doi.org/10.1016/S0008-8846(02)00958-4

[17] Rasheeduzzafar, O.S.B. Al-Amoudi, S.N. Abduljauwad, M. Maslehuddin, Magnesium-sodium sulfate attack in plain and blended cements, J Mater Civ Eng, 6 (1994) 201-222. https://doi.org/10.1061/(ASCE)0899-1561(1994)6:2(201)

[18] E.E. Hekal, E. Kishar, H. Mostafa, Magnesium sulfate attack on hardened blended cement pastes under different circumstances, Cem Concr Res, 32 (2002) 1421-1427. https://doi.org/10.1016/S0008-8846(02)00801-3

[19] C. Roosz, S. Grangeon, P. Blanc, V. Montouillout, B. Lothenbach, P. Henocq, E. Giffaut, P. Vieillard, S. Gaboreau, Crystal structure of magnesium silicate hydrates (MSH): The relation with 2: 1 Mg-Si phyllosilicates, Cem Concr Res, 73 (2015) 228-237. https://doi.org/10.1016/j.cemconres.2015.03.014

[20] B. Lothenbach, D. Nied, E. L'Hôpital, G. Achiedo, A. Dauzères, Magnesium and calcium silicate hydrates, Cem Concr Res, 77 (2015) 60-68. https://doi.org/10.1016/j.cemconres.2015.06.007

[21] E. Bernard, B. Lothenbach, I. Pochard, C. Cau-Dit-Coumes, Alkali binding by magnesium silicate hydrates, J Am Ceram Soc, 102 (2019) 6322-6336. https://doi.org/10.1111/jace.16494

[22] T. Zhang, L.J. Vandeperre, C.R. Cheeseman, Formation of magnesium silicate hydrate (MSH) cement pastes using sodium hexametaphosphate, Cem Concr Res, 65 (2014) 8-14. https://doi.org/10.1016/j.cemconres.2014.07.001

[23] M. Tonelli, F. Martini, A. Milanesi, L. Calucci, M. Geppi, S. Borsacchi, F. Ridi, Effect of phosphate additives on the hydration process of magnesium silicate cements, Journal of Thermal Analysis and Calorimetry, 138 (2019) 3311-3321. https://doi.org/10.1007/s10973-019-08847-9

[24] C. Sonat, W. Teo, C. Unluer, Performance and microstructure of MgO-SiO2 concrete under different environments, Const Build Mater, 184 (2018) 549-564. https://doi.org/10.1016/j.conbuildmat.2018.07.032

[25] T. Zhang, C. Cheeseman, L. Vandeperre, Development of low pH cement systems forming magnesium silicate hydrate (MSH), Cem Concr Res, 41 (2011) 439-442. https://doi.org/10.1016/j.cemconres.2011.01.016

[26] F. Winnefeld, E. Epifania, F. Montagnaro, E.M. Gartner, Further studies of the hydration of MgO-hydromagnesite blends, Cem Concr Res, 126 (2019) 105912. https://doi.org/10.1016/j.cemconres.2019.105912

[27] T. Zhang, T. Li, J. Zou, Y. Li, S. Zhi, Y. Jia, C.R. Cheeseman, Immobilization of Radionuclide 133Cs by Magnesium Silicate Hydrate Cement, Materials, 13 (2020) 146. https://doi.org/10.3390/ma13010146

[28] M.R. Marsiske, C. Debus, F. Di Lorenzo, E. Bernard, S.V. Churakov, C. Ruiz-Agudo, Immobilization of (Aqueous) Cations in Low pH MSH Cement, Applied Sciences, 11 (2021) 2968. https://doi.org/10.3390/app11072968

[29] D. Brew, F. Glasser, The magnesia-silica gel phase in slag cements: alkali (K, Cs) sorption potential of synthetic gels, Cem Concr Res, 35 (2005) 77-83. https://doi.org/10.1016/j.cemconres.2004.03.016

[30] S.A. Walling, H. Kinoshita, S.A. Bernal, N.C. Collier, J.L. Provis, Structure and properties of binder gels formed in the system Mg(OH)2-SiO2-H2O for immobilisation of Magnox sludge, Dalton Transactions, 44 (2015) 8126-8137. https://doi.org/10.1039/C5DT00877H

[31] T. Zhang, L.J. Vandeperre, C.R. Cheeseman, Magnesium-silicate-hydrate cements for encapsulating problematic aluminium containing wastes, Journal of Sustainable Cement-Based Materials, 1 (2012) 34-45. https://doi.org/10.1080/21650373.2012.727322

[32] L. Kidalova, E. Terpakova, N. Stevulova, MgO cement as suitable conventional binders replacement in hemp concrete, Pollack Periodica, 6 (2011) 115-122. https://doi.org/10.1556/Pollack.6.2011.3.11

[33] T. Zhang, E. Dieckmann, S. Song, J. Xie, Z. Yu, C. Cheeseman, Properties of magnesium silicate hydrate (MSH) cement mortars containing chicken feather fibres, Const Build Mater, 180 (2018) 692-697. https://doi.org/10.1016/j.conbuildmat.2018.05.292

[34] S.M. Evans, Novacem-carbon negative cement to transform the construction industry, Novacem slide deck presentation, Cambridge, Dec, 4 (2009) 2010.

[35] C. Kuenzel, F. Zhang, V. Ferrandiz-Mas, C. Cheeseman, E. Gartner, The mechanism of hydration of MgO-hydromagnesite blends, Cem Concr Res, 103 (2018) 123-129. https://doi.org/10.1016/j.cemconres.2017.10.003

[36] E. Gartner, M. Gimenez, V. Meyer, A. Pisch, A Novel Atmospheric Pressure Approach to the Mineral Capture of CO2 from Industrial Point Sources, Thirteenth annual conference on carbon capture, utilization and storage, Pittsburgh, Pennsylvania, (2014).

[37] N. Dung, A. Lesimple, R. Hay, K. Celik, C. Unluer, Formation of carbonate phases and their effect on the performance of reactive MgO cement formulations, Cem Concr Res, 125 (2019) 105894. https://doi.org/10.1016/j.cemconres.2019.105894

[38] G.B. Singh, C. Sonat, E. Yang, C. Unluer, Performance of MgO and MgO-SiO_2 systems containing seeds under different curing conditions, Cem Concr Compos, 108 (2020) 103543. https://doi.org/10.1016/j.cemconcomp.2020.103543

[39] D.R.M. Brew, F.P. Glasser, Synthesis and characterisation of magnesium silicate hydrate gels, Cem Concr Res, 35 (2005) 85-98. https://doi.org/10.1016/j.cemconres.2004.06.022

[40] D. Nied, K. Enemark-Rasmussen, E. L'Hopital, J. Skibsted, B. Lothenbach, Properties of magnesium silicate hydrates (MSH), Cem Concr Res, 79 (2016) 323-332. https://doi.org/10.1016/j.cemconres.2015.10.003

[41] E. Bernard, B. Lothenbach, C. Chlique, M. Wyrzykowski, A. Dauzères, I. Pochard, C. Cau-Dit-Coumes, Characterization of magnesium silicate hydrate (M-S-H), Cem Concr Res, 116 (2019) 309-330. https://doi.org/10.1016/j.cemconres.2018.09.007
[42] A. Pedone, F. Palazzetti, V. Barone, Models of Aged Magnesium-Silicate-Hydrate Cements Based on the Lizardite and Talc Crystals: A Periodic DFT-GIPAW Investigation, The Journal of Physical Chemistry C, (2017). https://doi.org/10.1021/acs.jpcc.7b00708
[43] W.-S. Chiang, G. Ferraro, E. Fratini, F. Ridi, Y.-Q. Yeh, U. Jeng, S.-H. Chen, P. Baglioni, Multiscale structure of calcium-and magnesium-silicate-hydrate gels, Journal of Materials Chemistry A, 2 (2014) 12991-12998. https://doi.org/10.1039/C4TA02479F
[44] C. Dewitte, A. Bertron, M. Neji, L. Lacarrière, A. Dauzères, Chemical and Microstructural Properties of Designed Cohesive MSH Pastes, Materials, 15 (2022) 547. https://doi.org/10.3390/ma15020547
[45] E. Bernard, B. Lothenbach, D. Rentsch, A. German, F. Winnefeld, Effect of carbonates on the formation of magnesium silicate hydrates, Materials and Structures, 55 (2022) 183. https://doi.org/10.1617/s11527-022-02018-3
[46] E. Bernard, B. Lothenbach, C. Cau-Dit-Coumes, I. Pochard, D. Rentsch, Aluminum incorporation into magnesium silicate hydrate (M-S-H), Cem Concr Res, 128 (2020) 105931. https://doi.org/10.1016/j.cemconres.2019.105931
[47] J. Szczerba, R. Prorok, E. Śnieżek, D. Madej, K. Maślona, Influence of time and temperature on ageing and phases synthesis in the MgO-SiO_2-H_2O system, Thermochimica Acta, 567 (2013) 57-64. https://doi.org/10.1016/j.tca.2013.01.018
[48] C. Roosz, P. Vieillard, P. Blanc, S. Gaboreau, H. Gailhanou, D. Braithwaite, V. Montouillout, R. Denoyel, P. Henocq, B. Madé, Thermodynamic properties of CSH, CASH and MSH phases: Results from direct measurements and predictive modelling, Applied Geochemistry, 92 (2018) 140-156. https://doi.org/10.1016/j.apgeochem.2018.03.004
[49] M. Kobayashi, K. Takahashi, Y. Kawabata, Physicochemical properties of the Portland cement-based mortar exposed to deep seafloor conditions at a depth of 1680 m, Cem Concr Res, 142 (2021) 106335. https://doi.org/10.1016/j.cemconres.2020.106335
[50] E. Bernard, B. Lothenbach, D. Rentsch, Influence of sodium nitrate on the phases formed in the MgO-Al_2O_3-SiO_2-H_2O system, Materials and Design, 198 (2021) 109391. https://doi.org/10.1016/j.matdes.2020.109391
[51] M. Vespa, C. Borca, T. Huthwelker, B. Lothenbach, R. Dähn, E. Wieland, Structural characterisation of magnesium (sodium) aluminium silicate hydrate (M-(N)-ASH) phases by X-ray absorption near-edge spectroscopy, Applied Geochemistry, 123 (2020) 104750. https://doi.org/10.1016/j.apgeochem.2020.104750
[52] E. Bernard, B. Lothenbach, F. Winnefeld, Magnesium (alumino) silicate hydrate formation in low-pH cement paste Proceedings of the 15th International Congress on the Chemistry of Cement (ICCC 2019) Prague, Czech Republic, 2019.
[53] S.A. Bernal, R. San Nicolas, R.J. Myers, R.M. de Gutiérrez, F. Puertas, J.S. van Deventer, J.L. Provis, MgO content of slag controls phase evolution and structural changes induced by accelerated carbonation in alkali-activated binders, Cem Concr Res, 57 (2014) 33-43. https://doi.org/10.1016/j.cemconres.2013.12.003
[54] R.J. Myers, B. Lothenbach, S.A. Bernal, J.L. Provis, Thermodynamic modelling of alkali-activated slag cements, Applied Geochemistry, 61 (2015) 233-247. https://doi.org/10.1016/j.apgeochem.2015.06.006
[55] S. Park, H.M. Park, H. Yoon, J. Seo, C.-M. Yang, J.L. Provis, B. Yang, Hydration kinetics and products of MgO-activated blast furnace slag, Const Build Mater, 249 (2020) 118700. https://doi.org/10.1016/j.conbuildmat.2020.118700
[56] S.M. Park, J. Jang, H.-K. Lee, Unlocking the role of MgO in the carbonation of alkali-activated slag cement, Inorganic Chemistry Frontiers, 5 (2018) 1661-1670. https://doi.org/10.1039/C7QI00754J
[57] S.A. Walling, S.A. Bernal, L.J. Gardner, H. Kinoshita, J.L. Provis, Phase Formation and Evolution in $Mg(OH)_2$-Zeolite Cements, Industrial & Engineering Chemistry Research, 57 (2018) 2105-2113. https://doi.org/10.1021/acs.iecr.7b04201
[58] Y. Jia, Y. Zou, X. Zou, Y. Jiang, F. Li, W. Ma, H. Yan, R. Hua, Effect of Aluminum incorporation on the Reaction Process and Reaction Products of Hydrated Magnesium Silicate, Frontiers in Materials, 8 (2022) 594. https://doi.org/10.3389/fmats.2021.810535
[59] C. Appelo, D. Postma, Geochemistry, Groundwater and pollution, 536 (2005). https://doi.org/10.1201/9781439833544
[60] J.C. Alt, D.A. Teagle, T. Brewer, W.C. Shanks III, A. Halliday, Alteration and mineralization of an oceanic forearc and the ophiolite - ocean crust analogy, Journal of Geophysical Research: Solid Earth, 103 (1998) 12365-12380. https://doi.org/10.1029/98JB00598
[61] E. Bernard, A. Dauzères, B. Lothenbach, Magnesium and calcium silicate hydrates, Part II: Mg-exchange at the interface "low-pH" cement and magnesium environment studied in a C-S-H and M-S-H model system, Applied Geochemistry, 89 (2018) 210-218. https://doi.org/10.1016/j.apgeochem.2017.12.006
[62] E. Bernard, B. Lothenbach, C. Cau-Dit-Coumes, C. Chlique, A. Dauzères, I. Pochard, Magnesium and calcium silicate hydrates, Part I: Investigation of the possible magnesium incorporation in calcium silicate hydrate (C-S-H) and of the calcium in magnesium silicate hydrate (M-S-H), Applied Geochemistry, 89 (2018) 229-242. https://doi.org/10.1016/j.apgeochem.2017.12.005
[63] L. de Ruiter, H. Austrheim, Formation of magnesium silicate hydrate cement in nature, Journal of the Geological Society, 175 (2018) 308-320. https://doi.org/10.1144/jgs2017-089
[64] C. Shi, J. Stegemann, Acid corrosion resistance of different cementing materials, Cem Concr Res, 30 (2000) 803-808. https://doi.org/10.1016/S0008-8846(00)00234-9
[65] E. Bernard, A. Jenni, M. Fisch, D. Grolimund, U. Mäder, Micro-X-ray diffraction and chemical mapping of aged interfaces between cement pastes and Opalinus Clay Applied Geochemistry, 115 (2020) 104538. https://doi.org/10.1016/j.apgeochem.2020.104538
[66] E. Bernard, B. Lothenbach, D. Rentsch, I. Pochard, A. Dauzères, Formation of magnesium silicate hydrates (M-S-H), Physics and Chemistry of the Earth, Parts A/B/C, 99 (2017) 142-157. https://doi.org/10.1016/j.pce.2017.02.005
[67] Z. Li, T. Zhang, J. Hu, Y. Tang, Y. Niu, J. Wei, Q. Yu, Characterization of reaction products and reaction process of MgO-SiO_2-H_2O system at room temperature, Const Build Mater, 61 (2014) 252. https://doi.org/10.1016/j.conbuildmat.2014.03.004
[68] R. Salomão, V. Pandolfelli, Efeito da adição de microssílica na hidratação de óxido de magnésio em concretos refratários (Microsilica addition as anti-hydration technique of magnesia in refractory castables), Cerâmica, 54 (2008) 43-48. https://doi.org/10.1590/S0366-69132008000100007
[69] H. Zhao, T. Hanein, N. Li, A. Alotaibi, A. Li, S. Walling, H. Kinoshita, Acceleration of MSH gel formation through the addition of alkali carbonates, Proceedings of the 15th International Congress on the Chemistry of Cement (ICCC 2019), Prague, 2019.
[70] Y. Jia, B. Wang, Z. Wu, J. Han, T. Zhang, L.J. Vandeperre, C.R. Cheeseman, Role of sodium hexametaphosphate in MgO/SiO_2 cement pastes, Cem Concr Res, 89 (2016) 63-71. https://doi.org/10.1016/j.cemconres.2016.08.003
[71] N. Dung, C. Unluer, Carbonated MgO concrete with improved performance: The influence of temperature and hydration agent on hydration, carbonation and strength gain, Cem Concr Compos, 82 (2017) 152-164. https://doi.org/10.1016/j.cemconcomp.2017.06.006
[72] H. Nguyen, H. Santos, H. Sreenivasan, W. Kunther, V. Carvelli, M. Illikainen, P. Kinnunen, On the carbonation of brucite: Effects of Mg-acetate on the precipitation of hydrated magnesium carbonates in aqueous environment, Cem Concr Res, 153 (2022) 106696. https://doi.org/10.1016/j.cemconres.2021.106696
[73] O.S. Pokrovsky, J. Schott, A. Castillo, Kinetics of brucite dissolution at 25 C in the presence of organic and inorganic ligands and divalent metals, Geochimica et Cosmochimica Acta, 69 (2005) 905-918. https://doi.org/10.1016/j.gca.2004.08.011
[74] B. Lothenbach, F. Winnefeld, Thermodynamic modelling of the hydration of Portland cement, Cement Concrete Research, 36 (2006) 209-226. https://doi.org/10.1016/j.cemconres.2005.03.001
[75] E. Bernard, B. Lothenbach, E. L'Hopital, D. Nied, A. Dauzeres, Magnesium silicate hydrates (M-S-H): formation kinetics and range of composition, 34th Cem Concr Sci Conf Sheffield, 2014, Paper No. W23.
[76] D. Kulik, T. Wagner, S.V. Dmytrieva, G. Kosakowski, F. Hingerl, K.V. Chudnenko, U. Berner, GEM-Selektor geochemical modeling package: revised algorithm and GEMS3K numerical kernel for coupled simulation codes, Computat Geochem, 17 (2013) 1-24. https://doi.org/10.1007/s10596-012-9310-6
[77] T. Thoenen, D. Kulik, Nagra/PSI chemical thermodynamic database 01/01 for the GEM-Selektor (V.2-PSI) geochemical modeling code, PSI, Villigen; available at http://gems.web.psi.ch/doc/pdf/TM-44-03-04-web.pdf , 2003.

[78] B. Lothenbach, D.A. Kulik, T. Matschei, M. Balonis, L. Baquerizo, B. Dilnesa, G.D. Miron, R.J. Myers, Cemdata18: A chemical thermodynamic database for hydrated Portland cements and alkali-activated materials, Cem Concr Res, 115 (2019) 472-506. https://doi.org/10.1016/j.cemconres.2018.04.018
[79] E. Bernard, B. Lothenbach, W.J. Zucha, U. Mäder, Stability of hydrotalcite (Mg-Al layered double hydroxide) in presence of different anions, Cem Concr Res, 152 (2022) 106674. https://doi.org/10.1016/j.cemconres.2021.106674
[80] B. Lothenbach, B. Xu, F. Winnefeld, Thermodynamic data for magnesium (potassium) phosphates, Applied Geochemistry, 111 (2019) 104450. https://doi.org/10.1016/j.apgeochem.2019.104450
[81] S. Miyata, The Syntheses of Hydrotalcite-Like Compounds and Their Structures and Physico-Chemical Properties-I: the Systems Mg^{2+}-Al^{3+}-NO_3^-, Mg^{2+}-Al^{3+}-Cl^-, Mg^{2+}-Al^{3+}-ClO_4^-, Ni^{2+}-Al^{3+}-Cl^- and Zn^{2+}-Al^{3+}-Cl^-, Clays and Clay Minerals, 23 (1975) 369-375. https://doi.org/10.1346/CCMN.1975.0230508
[82] S. Miyata, Anion-exchange properties of hydrotalcite-like compounds, Clays and Clay Minerals, 31 (1983) 305-311. https://doi.org/10.1346/CCMN.1983.0310409
[83] B. Xu, F. Winnefeld, B. Ma, D. Rentsch, B. Lothenbach, Influence of aluminum sulfate on properties and hydration of magnesium potassium phosphate cements, Cem Concr Res, 156 (2022) 106788. https://doi.org/10.1016/j.cemconres.2022.106788
[84] O. Pokrovsky, J. Schott, Surface chemistry and dissolution kinetics of divalent metal carbonates, Environmental science & technology, 36 (2002) 426-432. https://doi.org/10.1021/es010925u
[85] E. Gartner, T. Sui, Alternative cement clinkers, Cem Concr Res, 114 (2018) 27-39. https://doi.org/10.1016/j.cemconres.2017.02.002
[86] B. Panda, C. Sonat, E.-H. Yang, M.J. Tan, C. Unluer, Use of magnesium-silicate-hydrate (MSH) cement mixes in 3D printing applications, Cem Concr Compos, 117 (2021) 103901. https://doi.org/10.1016/j.cemconcomp.2020.103901
[87] T. Zhang, J. Zou, Z. He, L. Guo, Z. Wu, B. Wang, Chloride ion penetration resistance and pore structure of magnesium silicate hydrate (M-S-H) mortars, 1er international conference on Innovation in Low-Carbon Cement and Concrete technology (ILCCC) London, United Kingdom, 2019. https://doi.org/10.2991/icmea-17.2018.36
[88] S. Ruan, S. Liang, G. Kastiukas, W. Zhu, X. Zhou, Solidification of waste excavation clay using reactive magnesia, quicklime, sodium carbonate and early-age oven curing, Const Build Mater, 258 (2020) 120333. https://doi.org/10.1016/j.conbuildmat.2020.120333
[89] V. Shah, A. Scott, Use of kaolinite clays in development of a low carbon MgO-clay binder system, Cem Concr Res, 144 (2021) 106422. https://doi.org/10.1016/j.cemconres.2021.106422
[90] M. Dhakal, A.N. Scott, V. Shah, R.P. Dhakal, D. Clucas, Development of a MgO-metakaolin binder system, Const Build Mater, 284 (2021) 122736. https://doi.org/10.1016/j.conbuildmat.2021.122736
[91] V. Shah, A. Scott, Hydration and microstructural characteristics of MgO in the presence of metakaolin and silica fume, Cem Concr Compos, 121 (2021) 104068. https://doi.org/10.1016/j.cemconcomp.2021.104068
[92] V. Shah, Y. Dhandapani, A. Scott, Pore structure characteristics of MgO-SiO_2 binder, J Am Ceram Soc, 104 (2021) 6002-6014. https://doi.org/10.1111/jace.17971
[93] K. Scrivener, F. Martirena, S. Bishnoi, S. Maity, Calcined clay limestone cements (LC3), Cem Concr Res, 114 (2018) 49-56. https://doi.org/10.1016/j.cemconres.2017.08.017
[94] K. Khan, M.F. Ullah, K. Shahzada, M.N. Amin, T. Bibi, N. Wahab, A. Aljaafari, Effective use of micro-silica extracted from rice husk ash for the production of high-performance and sustainable cement mortar, Const Build Mater, 258 (2020) 119589. https://doi.org/10.1016/j.conbuildmat.2020.119589
[95] A. Tafraoui, G. Escadeillas, T. Vidal, Durability of the ultra high performances concrete containing metakaolin, Const Build Mater, 112 (2016) 980-987. https://doi.org/10.1016/j.conbuildmat.2016.02.169